

Self-propelled Chimeras

Nikita Kruk¹, Yuri Maistrenko^{1,2}, Nicolas Wenzel¹, and Heinz Koepl^{1,*}

¹*Department of Electrical Engineering and Information Technology,
Technische Universitaet Darmstadt, Darmstadt, Germany and*

²*Institute of Mathematics and Center for Medical and Biotechnical Research,
National Academy of Sciences of Ukraine, Kyiv, Ukraine*

(Dated: April 6, 2022)

We report the appearance of chimera states in a minimal extension of the classical Vicsek model for collective motion of self-propelled particle systems. Inspired by earlier works on chimera states in the Kuramoto model, we introduce a phase lag parameter in the particle alignment dynamics. Compared to the oscillatory networks with fixed site positions, the self-propelled particle systems can give rise to distinct forms of chimeras resembling moving flocks through an incoherent surrounding, for which we characterize their parameter domains. More specifically, we detect localized directional one-headed and multi-headed chimera states, as well as scattered directional chimeras without space localization. We discuss canonical generalizations of the elementary Vicsek model and show chimera states for them indicating the universality of this novel behavior. A continuum limit of the particle system is derived that preserves the chimeric behavior.

PACS numbers: 02.30.Ks, 05.10.-a, 05.45.Xt, 47.54.-r

Self-propelled particle (SPP) models have been widely investigated for the description of large variety of collective behavior, e.g. colonies of bacteria, swarms of insects, schools of fish, flocks of birds, human crowds, and interacting robots [1]. The Vicsek model [2] is considered to be the simplest model for this purpose, where the particle direction of motion is determined by the average direction of others within a given neighborhood, and the absolute velocity is constant. Classical results for the Vicsek model concern conditions for complete directional synchronization of the particles scattered in space. Recently, chimera states in oscillatory networks were discovered as remarkable spatio-temporal patterns where regions of synchrony coexist with regions of incoherent motion. First observed in 2002 for a non-locally coupled complex Ginzburg-Landau equation and for the Kuramoto model [3, 4], they today constitute a field of intensive theoretical and experimental research in physics, chemistry, and biology (see review paper [5] and references therein, and very recent contributions [6]).

We consider a modified version of the Vicsek model, where N particles move with a constant velocity in a two-dimensional space with periodic boundary conditions, according to the equations of motion of the form

$$\dot{r}_i = v(\varphi_i), \quad \dot{\varphi}_i = \frac{\sigma}{|B_\rho^i|} \sum_{j \in B_\rho^i} \sin(\varphi_j - \varphi_i - \alpha) \quad (1)$$

with $r_i = (x_i, y_i)$ and $v(\varphi_i) = (\cos \varphi_i, \sin \varphi_i)$, where the particles are assumed of unit mass and unit speed without loss of generality. Each particle i interacts with all neighbors j within a finite interaction range ρ , i.e. with all particles falling in the disk

$$B_\rho^i := \{j \mid (x_i - x_j)^2 + (y_i - y_j)^2 \leq \rho^2\}. \quad (2)$$

The alignment is controlled by the coupling coefficient σ and the time-dependent number of neighbors $|B_\rho^i|$. In

the alignment term in Eq. (1) we allow for a phase lag parameter α that induces eventually a circular motion of an aligned group of particles. For $\alpha = 0$, the dynamics of Eq. (1) coincides with the traditional Vicsek model in polar coordinates [7].

For model (1), we report the appearance of chimera states, where the particles stably split into two groups after a transient period: one phase-coherent and localized in space, the other phase-incoherent and space distributed. The states of this kind show unique properties that differ from “classical” chimeras in oscillatory networks with fixed node positions. In contrary, self-propelled chimeras in SPP systems refer to the local aggregation of a group of particles that then move coherently through space in an incoherent surrounding. A peculiarity of the dynamics is its diffusive character: some particles can sporadically leave the coherent group to behave in a disordered way, but others join it to move coherently. This fascinating behavior is preserved for natural extensions of the model (1) which are discussed later in this Letter. We emphasize that coherent structures in form of strips or blobs can also be obtained in the standard Vicsek model by introducing noise [8]. Our situation is radically different: coherent localized structures in Eq. (1) arise solely due to internal nonlinear interactions imposed by non-local coupling in the complete absence of noise.

Results of direct numerical simulation of model (1) in the two-parameter plane of coupling radius ρ and phase lag α are presented in the phase diagram in Fig. 1. It reveals the existence of chimera states in a considerable domain at an intermediate radius of coupling ρ and for a phase lag α between 1.2 and $\pi/2$. For smaller α or larger ρ , complete phase synchronization occurs, although the particle positions remain space-disordered as assigned by the initial particle distribution [9]. Alternatively, for α

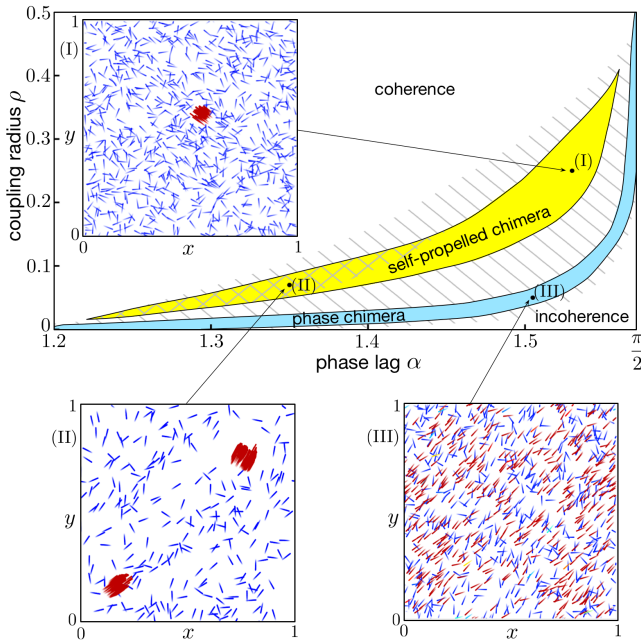


Figure 1. (Color online) Phase diagram for system (1) in the (α, ρ) parameter plane. Self-propelled and phase chimeras exist in yellow and blue regions, respectively; multi-headed chimeras are found in the cross-hatched region. Snapshots of typical regimes are shown in the insets: (I) and (II) self-propelled chimera, (III) phase chimera. Intermittent chaotic behavior is characteristic for neighboring regions (oblique hatching). Outside the aforementioned regions, complete phase synchronization (above) and full disorder (below) are observed. Snapshots are obtained starting from random initial conditions for (α, ρ) parameter tuples: (I) = (1.53, 0.25), (II) = (1.35, 0.08), (III) = (1.505, 0.05); color code corresponds to averaged phase velocity of the particles (see Fig. 2 captions and the text); $\sigma = 1.0$, $N = 1000$.

close to $\pi/2$ and small ρ collective motion is fully disordered both in phase and position [10].

Self-propelled chimeras with one coherent group exist for a large interval of phase lags (yellow parameter region in Fig. 1, snapshot (I)). Within a subdomain such one-headed chimeras co-exist with multi-headed chimeras comprising two or more separate coherent groups that move in a disordered surrounding (cross-hatched yellow region, snapshot (II)). Phase chimeras characterized by partial phase synchronization without any space localization can be observed for a distinct parameter domain of relatively narrow width (blue region, snapshot (III)). Finally, the domain encompassing those two distinct chimera regions corresponds to an intermittent system behavior between neighboring states resembling heteroclinic cycling (oblique hatched region). See Supplemental Material [11] and corresponding videos S1-S3 / [12] illustrating the reported chimera states starting from random initial conditions.

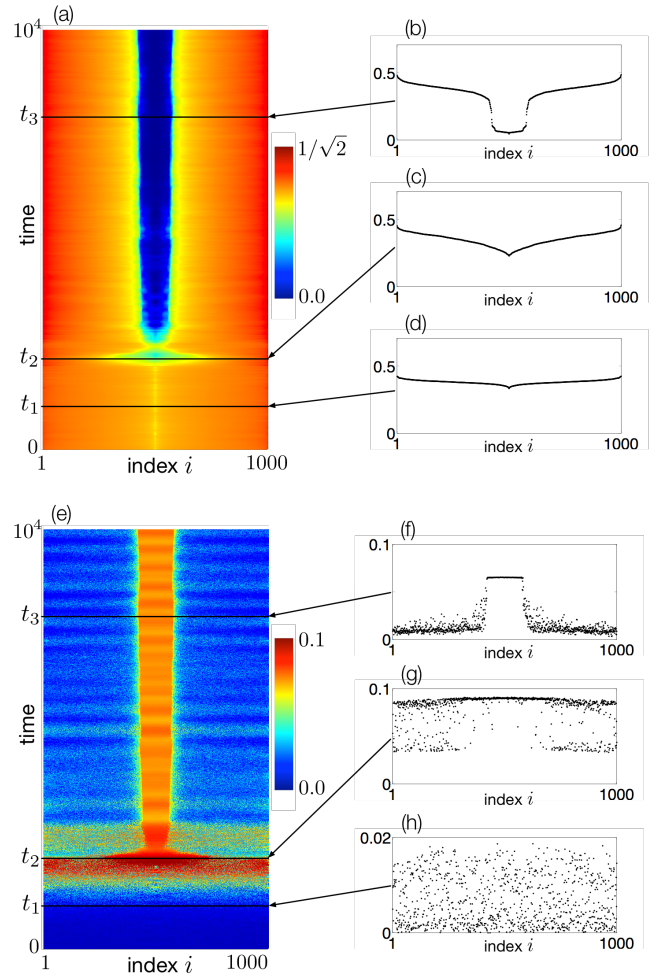


Figure 2. (Color online) Space-time plots for a chimera state in an SPP system characterized by means of localization (a) and phase velocity (e) measures (color coding). Localization is captured through the distance of particles to the point of maximal density. Phase velocity refers to the rate of change of direction φ of each particle. In both plots particles are ordered identically with respect to the distance to the maximal density point, with the particle of smallest distance placed in the center (see Section S.1 of [11] for an alternative representation); temporal averaging of 100 time units is applied; (b),(c),(d) and (f),(g),(h) instantaneous values of (a) and (e), respectively, at time units $t_1 = 1000$, $t_2 = 2100$, and $t_3 = 8000$, respectively; parameters: $\sigma = 1.0$, $\rho = 0.25$, $\alpha = 1.53$, $N = 1000$.

The typical emergence of chimera states in an SPP system is illustrated by the space-time plots in Fig. 2. The analysis demonstrates that particles in the coherent group create a phase synchronized cluster and that the remaining particles, not in the cluster, are phase desynchronized and scattered through the whole space. Along the route to this chimera state the following three characteristic phases are transversed starting from general ran-

dom initial conditions. First, within the initial transient period (cf. Fig. 2 at t_1) the system behavior is totally disordered both in space and in phase. Second, phase synchronization gradually accrues, however, there is no sign of particle localization (cf. Fig. 2 before t_2). Third, a transitional large group of phase coherent particles is formed (cf. Fig. 2 at t_2) and rapidly after, a self-propelled chimera state emerges that stays on for the rest of the simulation time (in Fig. 2 up to $t = 50000$).

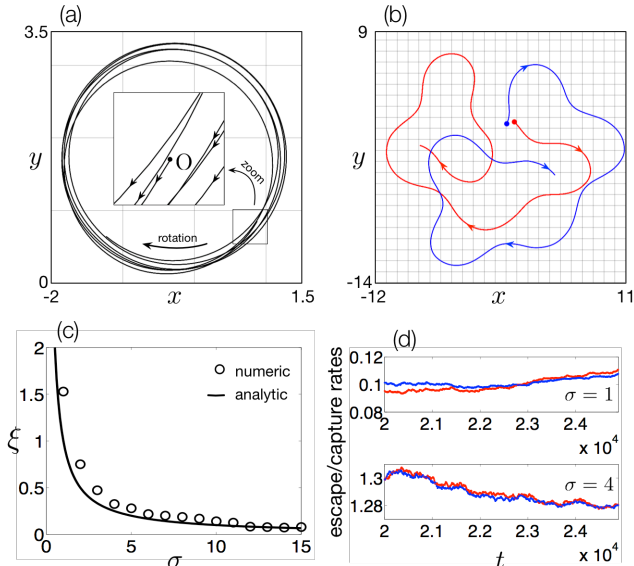


Figure 3. (Color online) Dynamics of a typical particle (a) in and (b) outside the coherent group for 500 time units (note different scales in (a) and (b), each grid box corresponds to the unit simulation box). Dots denote the starting points of tracing; (c) radius of rotation ξ of the coherent group as a function of the coupling coefficient σ : circles correspond to numerical simulations of Eq. (1), the solid line represents the analytical approximation through (3); (d) escape (red) and capture (blue) rates of the coherent group for $\sigma = 1$ and $\sigma = 4$ as average numbers of particles leaving and joining the cluster per unit time; $\rho = 0.25, \alpha = 1.53$.

Particles in the coherent group move along quasi-circular orbits (cf. Fig. 3(a)), clockwise for $\alpha > 0$ and counter-clockwise for $\alpha < 0$. The radius of the coherent group rotation ξ can be estimated, by analyzing Eq. (1) [13], as

$$\xi(\sigma) \approx \frac{1}{\sigma q \sin \alpha}, \quad (3)$$

where $q = \langle |N_c|/|B_\rho^i| \rangle_T$ is the time-average fraction of coherent particles N_c in the neighborhood B_ρ^i , calculated for every particle i in the cluster for the period of rotation T (in the case of Fig. 3 it is about 80 time units). As it follows from Eq. (3), the rotation radius ξ decreases with increase of the coupling strength σ and becomes

smaller than 0.5 for $\sigma > 3$ (see Fig. 3(c)). For this case, the coherent group moves entirely inside the unit square $[0, 1] \times [0, 1]$, i.e. without crossing periodic boundaries. See Supplemental Material [11] and videos S4 and S5 / [12] of the system behavior for $\sigma = 4$ and $\sigma = 10$, respectively. It demonstrates that, with increasing σ , localization of the coherent group decreases, so it covers larger but sparser area in the space.

Particles which are not in the coherent group scatter through the whole space exhibiting a kind of chaotic itinerancy, illustrated in Fig. 3(b). The desynchronized particles try to follow the circular rotations of the coherent group but generally fall off the cluster after some time and continue wandering again. Quasi-periodic and wandering intervals alternate in a chaotic manner resembling a homoclinic cycling. Occasionally, the particles can join the coherent group for longer time performing a number of full rotations. However, sooner or later, each of them will leave the coherent cluster. In Fig. 3(d), both escape and capture rates of the coherent cluster are shown illustrating a surprising balance between “evaporation” and “condensation”. As a result, the total number of particles in the cluster remains approximately constant. We note that the traditional phase order parameter [3] is limited in characterizing chimeras in SPP systems, especially for multi-headed chimeras (see Section S.2 of [11]).

Continuum Limit.—In the following we derive the continuum limit of the finite-particle model (1) and show by numerical integration of the phase component that partial phase synchronization as the necessary condition for chimeras is preserved in this limit. We follow the approach of [14] and start by defining the empirical probability density function for N particles

$$f^N(r, \varphi, t) = \frac{1}{N} \sum_{i=1}^N \delta(r_i(t) - r) \delta(\varphi_i(t) - \varphi). \quad (4)$$

Conservation of probability imposes a Vlasov-type equation of the form

$$\begin{aligned} \partial_t f^N(r, \varphi, t) = \\ - \nabla(\dot{r}(\varphi, t) f^N(r, \varphi, t)) - \partial_\varphi(\dot{\varphi}(r, \varphi, t) f^N(r, \varphi, t)). \end{aligned}$$

Under appropriate scaling and under mild regularity condition [15] the limiting distribution $f(r, \varphi, t) = \lim_{N \rightarrow \infty} f^N(r, \varphi, t)$ exists and satisfies correspondingly

$$\begin{aligned} \partial_t f(r, \varphi, t) = \\ - \nabla(\dot{r}(\varphi, t) f(r, \varphi, t)) - \partial_\varphi(\dot{\varphi}(r, \varphi, t) f(r, \varphi, t)), \end{aligned} \quad (5)$$

where $\dot{r}f$ is the flux due to the motion of the particles and $\dot{\varphi}f$ is the angular flux resulting from the alignment

mechanism

$$\dot{\varphi}(r, \varphi, t) = \frac{\sigma}{|B_\rho(r)|} \times \int_0^{2\pi} \int_{B_\rho(r)} dr' d\varphi' \sin(\varphi' - \varphi - \alpha) f(r', \varphi', t) \quad (6)$$

and the associated equation for $\dot{r}(\varphi, t)$ corresponding to (1). Accordingly, (5) is an integro-differential equation and delicate to solve numerically. Under a phase chimera state (cf. corresponding inset III in Fig. 1) we can assume spatial homogeneity [16] for all φ , yielding $f(r, \varphi, t) = \tilde{f}(\varphi, t)$ for the considered unit square domain. Integrating (5) over that domain yields

$$\partial_t \tilde{f}(\varphi, t) = -\sigma \partial_\varphi \left[\tilde{f}(\varphi, t) \int_0^{2\pi} d\varphi' \sin(\varphi' - \varphi - \alpha) \tilde{f}(\varphi', t) \right]. \quad (7)$$

According to inset III in Fig. 1 a phase chimera solution to (7) should exhibit a pronounced peak for a certain angle and significant nonzero mass at other angles corresponding to the coherent and non-coherent particles, respectively. For complete synchronization, in contrast, the phase distribution converges to a Dirac delta. Fig. 4 shows the solution of (7), based on a donor-cell advection scheme [17] with the use of minmod slope limiter, together with its global phase order parameter.

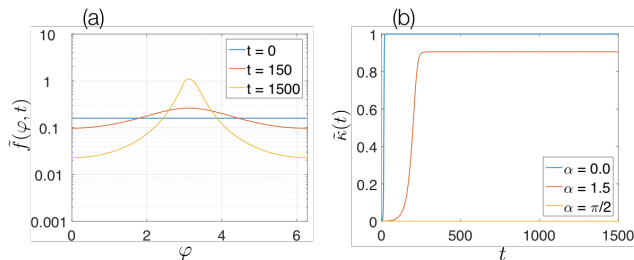


Figure 4. (Color online) Solution of the probability density function (7) of the continuum model; (a) log-plot of $\tilde{f}(\varphi, t)$ at different times for a phase chimera state for $\alpha = 1.5$; (b) time evolution of global order parameter $\tilde{\kappa}(t) = |\int_0^{2\pi} e^{-i\varphi} \tilde{f}(\varphi, t) d\varphi|$ for different phase lag parameters α .

To test if chimera states represent a universal behavior in SPP models, we also investigated an extended version of the modified Vicsek model (1) of the form

$$\begin{aligned} \dot{r}_i &= v(\varphi_i), \\ \dot{\varphi}_i &= \frac{\sigma}{|B_\rho^i|} \sum_{j \in B_\rho^i} G(\|r_j - r_i\|) \sin(\varphi_j - \varphi_i - \alpha) \\ &+ \mu \sum_{j \in B_\rho^i} F(\|r_j - r_i\|) \sin(\theta_{ji} - \varphi_i), \end{aligned} \quad (8)$$

where $\theta_{ji} = \arg(r_j - r_i)$ denotes the polar positional angle of particle j in the reference frame of particle i , G and F are general coupling functions of the scalar distance between particles. Compared to the minimal model (1), the first term on the right hand side of (8) replaces the piece-wise constant coupling function of (1). The second term on the right hand side of Eq. (8) describes arbitrary particle cohesion [18, 19], the strength of which is regulated by the parameter μ and the form of function F .

In the following example, the aligning force G is taken as a smooth approximation to the piece-wise constant function of (1) in the form $G(r) = 1$ if $r \leq \rho - \delta$, $G(r) = 0.5 - 0.5 \cos(\pi(r - \rho)/\delta)$ if $r < \rho$, and $G(r) = 0$ if $r \geq \rho$, where parameter $\delta > 0$ indicates the width of the transitional region [20]. Note that Eq. (8) turns into (1) as $\delta, \mu \rightarrow 0$. The attractive-repulsive force F is chosen to be a Morse-type potential $U(r) = C_R e^{-r/l_R} - C_A e^{-r/l_A}$, where coefficients $C_R, C_A > 0$ specify the ratio of repulsive and attractive forces and l_R, l_A encode their length scales, respectively [21–23].

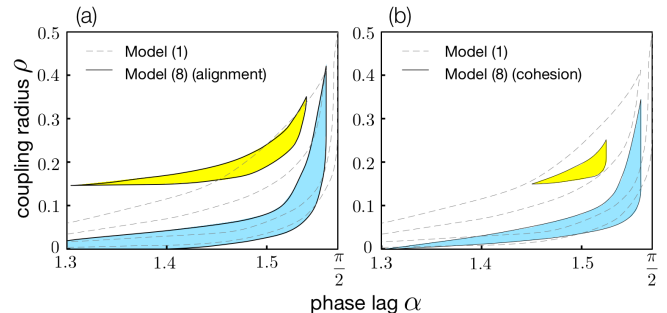


Figure 5. (Color online) Regions of self-propelled (yellow) and phase (blue) chimera states for model (8) with parameters (a) $\delta = 0.01, \mu = 0$ and (b) $\delta \rightarrow 0, \mu = 0.01$. Dashed lines indicate boundaries of the corresponding regions in the case of the basic model (1) presented in Fig. 1. Other model parameters: $C_R = 0.1, C_A = 0.001, l_R = 0.001, l_A = 0.1$.

Figure 5 shows that chimera states are preserved in the extended model (8) for small positive δ and μ , although the respective parameter regions change. In particular, the self-propelled chimera region (yellow in Fig. 1 and Fig. 5) shrinks rapidly whereas the phase chimera region (blue in Fig. 1 and Fig. 5) gradually expands for increasing δ and μ . Typical examples of the system behavior in this case are illustrated by videos (S6, S7) [12].

In conclusion, we have shown the existence of chimera states in a modified version of the Vicsek model. There are two types of chimera states: a localized directional state, where some number of particles assemble in a flock and move coherently together, and a scattered directional state, where the majority of particles synchronizes in phase but yet do not gather into a localized group. These

states exist for a wide range of coupling parameters. The transitions between different states occur through chaotic itinerancy when the system is captured by different attractors from the neighboring regions. We have described the behavior of the system in the case of the most striking one-headed self-propelled chimera state. We have derived the continuum limit for the proposed model, and shown that the joint condition for both types of chimera states, e.g. partial synchronization of phases, is preserved in this limit. We have found similar chimera-like regimes for a general SPP model including a cohesion term with both attractive and repulsive parts and assuming more realistic smooth phase alignment functions. This indicates a common, probably universal phenomenon, in SPP models of a new kind, due to the non-local phase lag interaction.

We are very grateful to Lutz Schimansky-Geier and Mark Timme for helpful discussions. Y.M. acknowledges support and hospitality of TU Darmstadt within the KIVA framework.

* Corresponding author.

heinz.koepl@bcs.tu-darmstadt.de

- [1] T. Vicsek and A. Zafeiris, *Physics Reports* **517**, 71 (2012).
- [2] T. Vicsek, A. Czirók, E. Ben-Jacob, I. Cohen, and O. Shochet, *Phys. Rev. Lett.* **75**, 1226 (1995).
- [3] Y. Kuramoto and D. Battogtokh, *Nonlinear Phenomena in Complex Systems* **5**, 380 (2002).
- [4] D. M. Abrams and S. H. Strogatz, *Phys. Rev. Lett.* **93**, 174102 (2004).
- [5] M. J. Panaggio and D. M. Abrams, *Nonlinearity* **28**, R67 (2015).
- [6] C. Bick and E. A. Martens, *New Journal of Physics* **17**, 033030 (2015); P. Ashwin and O. Burylko, *Chaos* **25**, 013106 (2015); L. Schmidt and K. Krischer, *Phys. Rev. Lett.* **114**, 034101 (2015); J. Xie, H.-C. Kao, and E. Knobloch, *Phys. Rev. E* **91**, 032918 (2015); L. Larger, B. Penkovsky, and Y. Maistrenko, *Nature Communications* **6**, 7752 (2015); Y. Maistrenko, O. Sudakov, O. Osiv, and V. Maistrenko, *New Journal of Physics* **17**, 073037 (2015); I. Omelchenko, A. Provata, J. Hizanidis, E. Schöll, and P. Hövel, *Phys. Rev. E* **91**, 022917 (2015); S. Olmi, E. A. Martens, S. Thutupalli, and A. Torcini, *Phys. Rev. E* **92**, 030901 (2015).
- [7] A. Chepizhko and V. Kulinskii, *Physica A: Statistical Mechanics and its Applications* **389**, 5347 (2010).
- [8] H. Chaté, F. Ginelli, G. Grégoire, F. Peruani, and F. Raynaud, *The European Physical Journal B* **64**, 451 (2008); A. P. Solon, H. Chaté, and J. Tailleur, *Phys. Rev. Lett.* **114**, 068101 (2015); K. H. Nagai, Y. Sumino, R. Montagne, I. S. Aranson, and H. Chaté, *Phys. Rev. Lett.* **114**, 168001 (2015).
- [9] This phase synchronized regime is characteristic for the standard Vicsek model ($\alpha = 0$), it persists in our model for all $\alpha < \pi/2$ if the coupling radius is large ($\rho > 0.4$).
- [10] Chimera states in model (1) are obtained for attractive coupling, which is given by a phase lag parameter $\alpha < \pi/2$. In the repulsive coupling case, $\alpha > \pi/2$, the behavior becomes globally disordered both in phase and position. Nevertheless, under some more general conditions, the Vicsek model with an anti-alignment interaction may produce orientationally ordered states and periodic vortex arrays [18].
- [11] See Supplemental Material at [URL will be inserted by publisher] for alternative space-time plots with single global ordering (Section S.1), for global and local order parameters (Section S.2), and for descriptions of videos [12] (Section S.3).
- [12] See https://www.youtube.com/playlist?list=PLjL7stT6PH4x1qpj_fFa2Rx5bI6Eyg0uw for videos illustrating the reported chimera states starting from random initial conditions.
- [13] Due to the fact that every particle of the coherent group has the same frequency characteristic (see Fig. 2), the evolution of the direction of motion (1) can be transformed into the combination of coherent and incoherent parts as $\dot{\varphi}_i = -\sigma \sin(\alpha) |N_c| / |B_\rho^i| + \sigma / |B_\rho^i| \sum_{j \in B_\rho^i \setminus N_c} \sin(\varphi_j - \varphi_i - \alpha)$. As particles move along circular trajectories, their speed values are determined as $\|v_i\| = \xi_i \dot{\varphi}_i$. Thus, using both equalities leads to (3).
- [14] D. S. Dean, *Journal of Physics A: Mathematical and General* **29**, L613 (1996).
- [15] H. Spohn, *Large Scale Dynamics of Interacting Particles*, 1st ed. (Springer, 1991).
- [16] F. Peruani, A. Deutsch, and M. Bär, *The European Physical Journal Special Topics* **157**, 111 (2008).
- [17] C. B. Laney, *Computational Gasdynamics* (Cambridge University Press, Cambridge, New York, NY, 1998).
- [18] R. Großmann, P. Romanczuk, M. Bär, and L. Schimansky-Geier, *Phys. Rev. Lett.* **113**, 258104 (2014).
- [19] G. Grégoire and H. Chaté, *Phys. Rev. Lett.* **92**, 025702 (2004).
- [20] There are numerous possible functional forms [24] that satisfy such a gradual transitional switching between the levels 1 and 0, we consider one of them, proposed in [25]. In such forms, the switching is activated at the distance δ to the originally sharp transition point $r = \rho$ such that strength of interaction gradually decreases from 1 to 0 as r goes through the interval $(\rho - \delta; \rho)$.
- [21] J. A. Carrillo, Y. Huang, and S. Martin, *European Journal of Applied Mathematics* **25**, 553 (2014).
- [22] M. R. D'Orsogna, Y. L. Chuang, A. L. Bertozzi, and L. S. Chayes, *Phys. Rev. Lett.* **96**, 104302 (2006).
- [23] H. Levine, W.-J. Rappel, and I. Cohen, *Phys. Rev. E* **63**, 017101 (2000).
- [24] P. J. Steinbach and B. R. Brooks, *Journal of Computational Chemistry* **15**, 667 (1994).
- [25] J. Tersoff, *Phys. Rev. B* **39**, 5566 (1989).